Hierarchical Diffusion Tensor Image Registration Based on Tensor Regional Distributions

P. YAP[1], H. ZHU[2], W. LIN[1], AND D. SHEN[1]

[1]DEPARTMENT OF RADIOLOGY AND BRIC, UNIVERSITY OF NORTH CAROLINA, CHAPEL HILL, NORTH CAROLINA, UNITED STATES, [2]DEPARTMENT OF BIOSTATISTICS AND BRIC, UNIVERSITY OF NORTH CAROLINA, CHAPEL HILL, NORTH CAROLINA, UNITED STATES

INTRODUCTION: Diffusion tensor imaging (DTI) is capable of non-invasively measuring water diffusion in vivo. While DTI has been widely employed to delineate potential white matter abnormality in different neurological diseases, registration of diffusion tensor images across different subjects is a critical prerequisite for detailed statistical analysis on voxel-by-voxel basis. However, spatial normalization of diffusion tensor images is challenging both technically and computationally given that tensor data representation is high dimensional in nature, and thus it requires not only to spatially warp, but also to appropriately reorient the tensor at each voxel. Conventional DTI registration methods generally extract tensor scalar features from each tensor as such to construct scalar maps. Subsequently, regional integration and other operations such as edge detection can be performed to extract more features to guide the registration. There are, however, two major limitations with these approaches. First, the computed regional features might not reflect the actual regional tensor distributions. Second, by the same token, gradient maps calculated from the tensor-derived scalar feature maps might not represent the actual tissue tensor boundaries. To overcome the two major limitations associated with the currently available approaches, a new approach is proposed by performing regional computation and edge detection directly on the tensors. Regional tensor distribution information, such as mean and variance, is computed in a multiscale fashion directly from the tensors by taking into account voxel neighborhood of different sizes, and hence capturing tensor information at different scales, which in turn can be used to hierarchically guide the registration. Such multiscale scheme can help alleviate the problems of trapping in a local minimum. Regional information is also more robust to noise since one can better determine the statistical properties of each tensor by taking into account the properties of its surrounding, mitigating the effect of noise. Also incorporated in our method is edge information extracted directly from tensors, which is crucial to facilitate registration of tissue boundaries. Detailed descriptions of this new approach are provided below.

METHOD AND RESULTS: **Tensor Regional Distributions**: For each voxel in diffusion tensor images, multi-scale regional tensor distribution information was extracted from its multi-scale neighborhoods. Specifically, for a given tensor D(x, y, z), the regional tensor distribution information was extracted from its neighborhood {D(u, v,w)|(u, v, w) $\in$ N(x, y, z)}. By varying the size of N(x, y, z) or by scaling the image itself, a rich set of multi-scale tensor regional distribution information could be obtained and employed to drive the registration hierarchically. To avoid tensor computation in a curved space, we took the matrix logarithm of all the original tensors, i.e., log(D(x, y, z)), for all (x, y, z). The tensor regional mean and variance for each voxel were then computed in the log-space. **Tensor Edges**: To better extract tissue boundaries, we extended Canny edge detector to work directly on diffusion tensor images instead of their scalar maps. Canny edge detector can be used to extract image gradient boundaries, and is robust to noise due to the employment of Gaussian filter to smooth out the noise prior to edge detection. For fast edge detection, 3D Gaussian-based image filtering was implemented using three subsequent steps of 1D Gaussian filtering along the x, y, and z directions independently. This was then followed by gradient map computation and non-maximum suppression in the 3D space. Note that edge detection was performed in the log-space. **Hierarchical Deformable Registration**: For each voxel, features obtained above were grouped into an attribute vector. As shown in Fig. 1, these attribute vectors are rich enough to permit discrimination of different brain anatomical structures. For computation efficiency, a subset of voxels with distinctive attribute vectors was selected as the set of *driving voxels*, providing temporary landmarks for correspondence matching. The initial driving voxels were employed to obtain a more reliable starting registration, facilitating relatively less distinctive driving voxels during later stages of the registration. The brain volume was deformed in a non-linear hierarchical fashion similar to that in [1]. **Simulated Deformation Fields**: We generated 20 simulated deformation fields, which served as the ground truth, using the statistical model of deformation (SMD) proposed in [2]. Using a set of brain images as the template, 20 simulated brain images can be constructed, which were then registered back onto the template using the proposed method. Registration accuracy can then be evaluated by comparing the deformation fields with the ground truth. The average Euclidean distance deformation field error given by the proposed method is 0.67 voxel (std: 0.43), indicating a subvoxel registration accuracy. In comparison, Yang et al.'s method which was tested using a similar dataset [3], reported a mean error of 0.86 voxel; the proposed method yields more than 20% improvement. **Fiber Tractography**: Using FACT [4], fiber bundles passing through two ROIs (see Fig. 2) were tracked, extracted, and compared for quantifying registration accuracy in these specific regions. Using a measure similar to that referred to as the *mean of the closest distances* in [5], errors given by the proposed method are 0.62mm and 0.77mm (stds: 0.16 & 0.07) for the genu and splenium fibers, respectively. The rather small errors with our approach signify good registration accuracy. **Atrophy Simulation**: We introduced atrophy on the simulated brains, by modifying the tensors in the selected region to be more isotropic (Fig. 3). After registering them onto the template, we tested whether the atrophic region was still detectable using paired *t*-test. The results are shown in Fig. 3. The average *t* values for affine registration and our method are 4.26 and 9.91, respectively. **Real Data**: 21 brain images of real subjects were registered onto a randomly selected template and an average image was generated from the registered images. The FA edge map of the average image, superimposed on the FA map of the template image (Fig. 4), indicates good consistency between their FA maps.

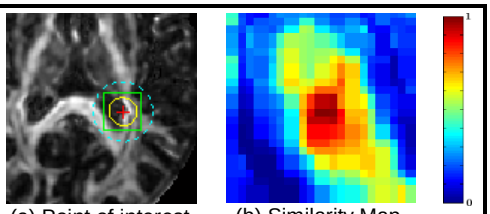

(a) Point of interest (b) Similarity Map

Fig. 1 Distinctiveness of attribute vectors. The attribute vector of the point of interest in (a) is compared with other points in the image volume. The similarity map for the region inside the green box is magnified and shown in (b).

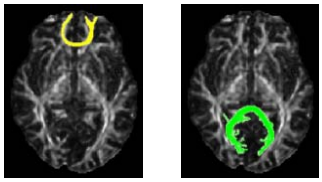

Fig. 2 Fiber bundles in genu (left) and splenium (right).

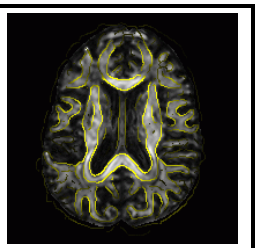

Fig. 4 FA edge map of the group-averaged tensor image superimposed on template FA map.

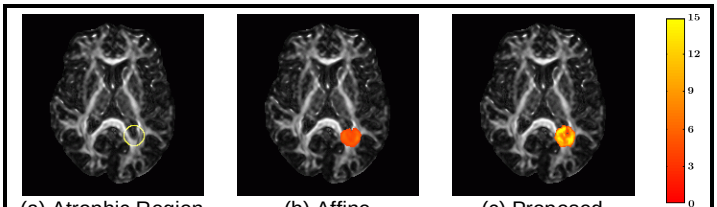

(a) Atrophic Region (b) Affine (c) Proposed

Fig. 3 Paired *t*-test between control and atrophic brain images.

REFERENCES: [1] D. Shen et al., *IEEE TMI*, 21(11), 1421–1439, 2002. [2] Z. Xue et al., *Neuroimage*, 33(3), 855–866, 2006. [3] J. Yang et al., *SPIE Med. Imaging'08*, 2008. [4] S. Mori et al., *A. Neurology*, 47(2), 265–269, 1999. [5] G. Gerig et al., *IEEE EMBS*, 4421–4424, 2004.